J Mater Sci (2008) 43:5891–5897
DOI 10.1007/s10853-008-2853-1

Impact of beta radiation on the strength of *Steatoda triangulosa* spider silk

E. M. Pogozelski · D. C. Abramo · L. Papasergi · B. D. See · C. M. Kieffer · S. J. Padalino

Received: 17 November 2007 / Accepted: 1 July 2008 / Published online: 31 July 2008

Abstract Silk from the spider *Steatoda triangulosa* is harvested, and samples are subjected to various doses of beta radiation using a scanning electron microscope (SEM). Irradiated and unirradiated samples are destructively tested to determine the stress–strain characteristics. From these data, the strength of the irradiated silk is determined as a function of dose.

Background

Dragline silk from the house spider *Steatoda triangulosa* is used at the Omega Laser at the University of Rochester Laboratory for Laser Energetics (LLE). The silk physically supports Inertial Confinement Fusion (ICF) fuel targets both during the fuel-filling process and during irradiation by the laser beams [1, 2]. Empty ICF targets are mounted onto four pieces of dragline silk, and the assembly is immersed in a Deuterium/Tritium (DT) gas of controlled pressure and temperature. The pressure is increased over several days to fill the target with fuel via diffusion, while the temperature is reduced to allow the DT gas to solidify inside the target. The maximum pressure reaches approximately 1000 atm [3], and the total absorbed dose for cryo-DT targets is estimated to be approximately 100 Mrad (T. Craig Sangster and M. Bonino, pers. comm.). Our goal is to confirm that the silk will maintain sufficient strength in this tritium-rich environment and in higher-dose environments to continue to support the weight of the target (about 0.6 μN).

There are several advantages in using silk from the *Triangulosa* species of cobweb spiders. The spiders are common and harmless. They can live in captivity for several years. Unlike spiders that only eat prey trapped in their webs, the *Triangulosa* spiders actively chase prey, allowing us the convenience of using flightless fruit flies for food.

Additionally, *Triangulosa* spider silk itself is very appropriate for the research at LLE. It is small (each strand having a diameter of about a micron), and therefore low-mass, minimizing contamination in the shot chamber. In contrast to other spiders we have examined that generate dragline silk made of 50 or more strands, the *Triangulosa* dragline consists of exactly two parallel cylindrical strands joined together lengthwise. This pair has a somewhat flat cross section, which is convenient for mounting the silk to the spherical targets. The consistency of the number of strands in the *Triangulosa* dragline also permits accurate computation of the stress of the silk, which depends on the cross-sectional area of the sample.

Harvesting

Approximately two dozen spiders are kept in Geneseo's spider silk lab at any given time. Silk is harvested in a manner similar to that used at the Omega lab [4]. A female spider is held in an open Petri dish, and allowed to descend freely. The spider connects her dragline to the dish, and descends (at an uncontrolled rate; the speed of descent may vary from 5 to 20 cm/s). The spider descends until about 1.3 m of silk has been obtained. During the descent, there is a chance that the spider will stop and then climb her own

E. M. Pogozelski (✉) · D. C. Abramo · L. Papasergi · B. D. See · C. M. Kieffer · S. J. Padalino
SUNY Geneseo, Geneseo, NY 14454, USA
e-mail: pogo@geneseo.edu

dragline back up to the starting Petri dish. Since this retreat happens only near the bottom of a descent, it was hypothesized that when the dragline becomes long, the spider visually searches for a landing surface, and returns upwards when none seems available to her. To prevent this upwards retreat, a second plastic dish is held below the spider as she descends, at a constant separation of about 2 cm. The spider continues to descend as long as she sees this potential landing site nearby. At the end of the descent, the spider is allowed to land in another Petri dish.

At this instant, the sample consists of a vertical dragline segment, connected to two Petri dishes (one at the top, and one at the bottom). This group is moved as a unit so that the dragline segment makes contact with two narrow stationary horizontal aluminum rods, separated by a vertical distance of 1.2 m. The silk is allowed to adhere to these rods, which are coated with double-sided tape to increase adhesion. Once the dragline is attached to these rods, the Petri dishes are no longer needed and are set aside.

Next, the dragline is wrapped onto a temporary carousel (Fig. 1). The carousel is an aluminum disc of diameter 9 cm, to which six spokes are attached. The spokes point in the same direction as the axis of the main carousel disc, and are circumferentially arranged, having a length of 5 cm and a diameter of 3 mm each. The distance between adjacent spokes is 4 cm, and a typical harvest produces about a dozen of 4-cm samples between these spokes. Of these, two samples are used to make measurements of the strand diameter, five are tested for strength without being irradiated, and five are irradiated prior to strength testing. It is not unusual for 1 or 2 of the 12 samples to break during handling and transportation, reducing the total number of samples from the harvest.

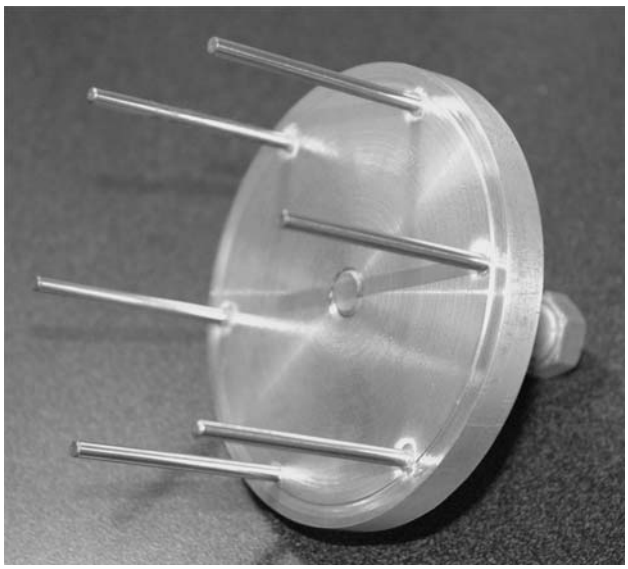

Fig. 1 Carousel used to harvest dragline silk. The spokes are 30 mm apart. A continuous section of dragline is wound around this carousel, isolating 12–15 shorter silk segments between the six spokes seen here

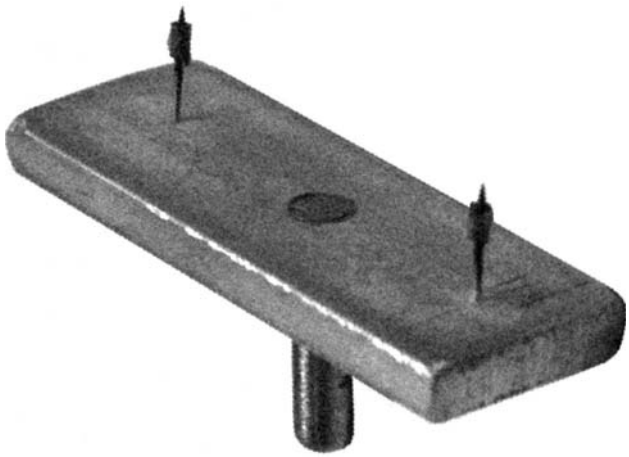

Fig. 2 Transport fixture with a mounted silk sample. This fixture doubles as the SEM cathode during both irradiation and imaging of the silk. Although the 0.45-mm steel pins and mounting tubes are visible, the silk is too fine to see in this image

To prepare an individual dragline sample for testing, it is first moved to a transport fixture, which allows for easy handling and manipulation of a single strand (Fig. 2). The transport fixture is an aluminum plate with two small steel pins (7 mm long, 0.45 mm diameter) separated by 25 mm. A hollow steel tube (2 mm long, 0.50 mm inner diameter, 1.0 mm outer diameter) is slid onto each pin. The carousel is then placed near the transport fixture so that a single silk sample touches each of the two hollow pins. A drop of cyanoacrylate is added to bind the silk to each tube, and the ends of the sample are cut with scissors from the carousel. The glue is allowed to cure for 24 h, during which time the sample is refrigerated to minimize moisture absorption by the silk.

During handling and preparation, the silk is unavoidably stretched. However, this does not seem to alter the maximum strength of the sample since experiments with a single piece of silk indicate that subsequent stress–strain results are independent of prior stressing (assuming, of course, that the silk is not broken during a test).

Determination of diameter

Of the dozen samples prepared in this way from a single harvest, two are used solely for determination of the strand diameter. Throughout this article, "diameter" refers to the diameter of only one of the two cylindrical silk strands that comprise a single dragline, rather than referring to the size of the combined dragline. The accuracy of the diameter affects both the computation of the stress and the computation of the irradiation dose. The silk diameter is measured using a Scanning Electron Microscope (SEM). The transport

fixture mounts directly into the SEM, and acts as the cathode for the electron beam. SEM images of the silk are generally fairly indistinct, due to the small size of the silk, due to blurring of the image as the silk moves because of thermal effects from the electron beam, and due to relatively poor contrast with the background. To improve the clarity and contrast of the image, the silk is plated with a few atoms' thickness of gold/palladium alloy before being imaged by the SEM. Since the size of a layer of gold is about 0.13 nm, a ten atom layer of gold will increase the diameter by 2.3×10^{-3} microns, which is 0.2% of the silk diameter and considerably less than the uncertainty on our measurements. The clarity of the SEM images is greatly improved as a result of the plating. Samples being stress tested are not plated.

The diameter of each strand is determined in five locations, resulting in variations in the diameter as high as 10%. Despite the gold plating, determination of the diameter is problematic because of shadows and edge effects on the SEM image. Some human judgment is necessary to identify the edges of the strand on an image. To resolve this problem, we apply a layer of latex microspheres to the transport fixture prior to SEM imaging. The microspheres have a known diameter of 0.80 ± 0.01 microns, which is similar to the diameter of the silk. Both the microspheres and the silk are visible in the SEM image, and have a similar appearance across any diameter (Fig. 3). The double-stranded nature of the silk (oriented vertically in the image) is evident, with microspheres visible on either side of the dragline. Direct measurements of the diameter of the microspheres using the SEM images resulted in a diameter of 0.91 ± 0.11 mm, which is 14% larger than the known size of the spheres. The discrepancy is primarily due to the presence of shadows and blurred edges on the SEM image. Therefore, the size of the silk as measured on the SEM was assumed to be oversized by this factor. After this adjustment, the average diameter of a strand is found to be 0.93 microns, with a standard deviation of 0.14 microns. This compares well with Bonino's result of 1.00 ± 0.21 microns [4]. It should be noted that the size and strength of the harvested silk, being biologically generated, is dependent on the size of the animal as well as many other factors [5].

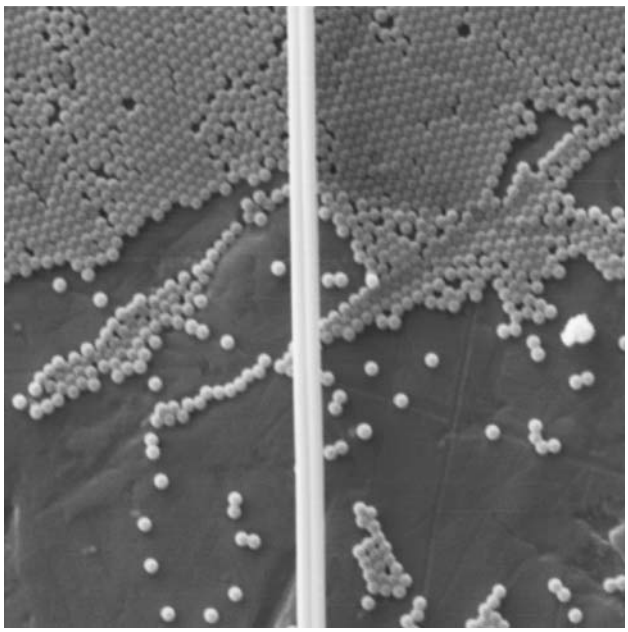

Fig. 3 SEM image (40 microns × 40 microns) of a segment of dragline silk with 0.8 micron microspheres visible in the background. The double-stranded nature of the silk is evident. The substrate is aluminum

Additionally, attempts were made to determine the diameter using optical microscopes, but the results were significantly worse due to various issues related to diffraction (the diameter of the silk is comparable to that of visible light), shadowing, and focus.

CASINO simulation

At the Omega facility, the spider silk is irradiated by prolonged exposure to tritium, which emits beta particles over a range of energies up to 18 keV, with an average energy of 6.5 keV. The dose absorbed by the silk is around 100 Mrad [3]. To verify that it is reasonable to compare irradiation from an SEM with exposure to tritium, we modeled the spider silk using the CASINO ("Monte CArlo SImulation of ElectroN Trajectory in Solids") simulation software [6]. CASINO requires the elemental composition and density of the target. For our silk, the composition was assumed to be 51% hydrogen, 24% carbon, 17% oxygen, and 8% nitrogen by number, based on amino acid analysis of dragline silks from a variety of other spider species [7].

Density is not directly measured in this study; instead, various literature was consulted to determine the density of the silk. Bonino [4] reports that the density of *Triangulosa* dragline silk is 1200 kg/m^3. Other sources [8, 9] report that dragline silk for a variety of different spider species ranges from 1250 to 1350 kg/m^3. For the current study, the density is assumed to be 1200 kg/m^3, since the Bonino study uses the same spider and silk type.

In CASINO, the target can only be modeled as a two-dimensional semi-infinite plane, impacted by a point beam of mono-energetic electrons. Our simulation used 2000 unit cells. The output is the distribution of energy deposition in the target, with darker cells indicating higher energy deposition (Fig. 4). In this figure, the incident beam is directed vertically downwards, and strikes the target material in the center of its upper surface. The average energy penetration is seen to be about 350 microns.

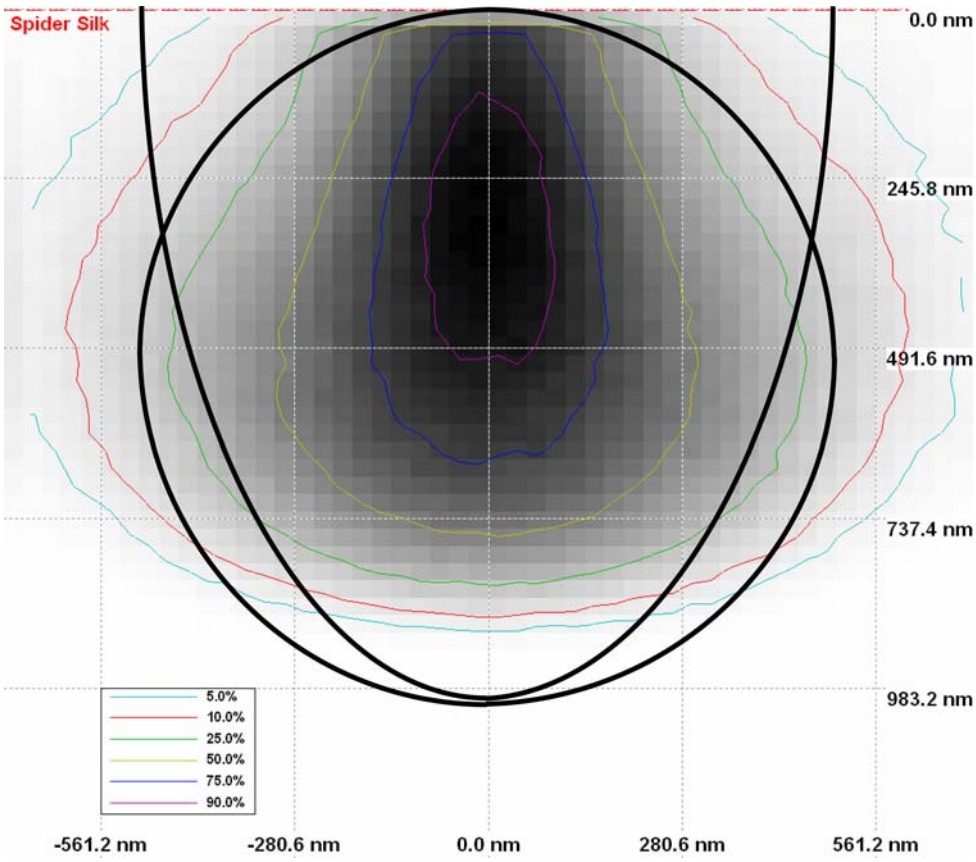

Fig. 4 CASINO results for 5 keV electrons. Darker regions indicate higher energy deposition, and deposition is integrated over the area of the silk sample. The 1.0 micron diameter circle shows the scale of a typical piece of silk. Since the upper boundary of the simulation is flat, the silk sample is modified to the half-ellipse shown, which has the same vertical thickness (as a function of horizontal position) as the circular contour. For the computation shown, 99% of the electron energy is deposited within the elliptical contour

Depending on the electron energy, the incident dose is not necessarily the same as the absorbed dose. Since silk is not a semi-infinite flat plane, and the tritium radiation is incident from multiple sides rather than a single point, it was necessary to approximate the deposition rates within a spatial region comparable to a real strand of silk. A quick approximation would be to compute the total energy deposited within a circular region adjacent to the edge of the semi-infinite plane. However, CASINO predicts that some energy is deposited in the semi-infinite plate above the circular region of interest, which is a non-physical result.

To attempt to match the flat-plate nature of the CASINO model to the real silk, the energy deposition was not determined within the circular region, but was instead determined within a semi-elliptical region having the same thickness as the circular region at each horizontal station. This model provides more conservative results than the circular profile (Fig. 4).

Using a "typical" diameter of 1 micron, the fraction of electron energy deposited within the silk was determined for several energies. Since our SEM is capable of only three discrete electron energies (5, 10, and 15 keV), these energies (along with the 6.5 keV average energy of tritium) were the only energies modeled in CASINO. The primary result of this analysis was that higher energies pass through the target with a smaller likelihood of depositing energy within the first micron of the target. For 6.5 keV electrons, the deposited dose rate in the semi-elliptical target was 96.5%. For 5.0 keV electrons, the deposited dose was 100.0%, while for 10.0 keV electrons, the deposited dose was 47.6%, and for 15.0 keV electrons, the deposited dose was only 18.6%. Therefore, to ensure that the use of the SEM for irradiation was sufficiently conservative, the 5 keV SEM energy was chosen.

Irradiation and dose determination

Beta irradiation of the silk takes place in the SEM. Unlike the tritium dose at LLE, which irradiates the silk from all sides, our silk is irradiated from one side only. However, if the deposition rate is 100%, the results should be comparable. The SEM irradiates a square area of side w. The dose in rads (energy per unit mass) incident on the two cylindrical elements of the silk is computed from the energy E of the SEM, the current I of the electron beam, the time of exposure t, the density ρ of the silk, radius r of the silk, and the area w^2 of the exposed SEM cathode, as well as the fundamental charge e, according to:

$$\text{Dose} = \frac{2EIt}{\rho\pi rew^2} \quad (1)$$

If 100% of the incident energy is deposited in the silk, this is equal to the absorbed dose. To achieve a desired dose, the exposure time is varied while the current is held constant. A typical exposure will require less than 10 min, but naturally depends on the desired dose.

The current passing through the SEM base is measured directly. However, because the beam liberates electrons from the SEM base, the measured current is smaller than the beam current exposing the silk. To calibrate the current measurements, a Faraday Cup was used to recapture the liberated electrons, and the ratio of the actual beam current to the measured current was determined to be 1.88. Of the electrons liberated from the base, virtually none contribute to the dose of the silk, since the silk is a few thousand diameters away from the base.

The entire strand of silk is not irradiated; instead, only the segment visible in the SEM is irradiated. This length, w, is typically 600 μm. This has the unfortunate side effect that subsequent strain rates will be difficult to interpret, since they are the combination of the strains of both the irradiated and unirradiated portions of the silk. Fortunately, the force in any silk sample is constant in all parts of the sample, irradiated or not, so that the measurements of dragline strength are not dependent on the fraction of the sample that is irradiated.

To examine whether irradiation from only a single side of the silk produces a different result than irradiation from multiple sides, a set of experiments were conducted in which silk was irradiated from two sides. A single harvest was divided into ten samples. As a control, five of these samples were irradiated from a single side, as usual. The remaining samples were irradiated at half the dose of the control samples. Then, they were rotated by 180° and irradiated again at half the dose of the control samples, so that the total dose was the same. Fiducial marks on the SEM mount were used to ensure that the SEM was exposing the top and bottom of the same part of the strand for each half-dose. Full doses ranged from 30 to 240 Mrad. Finally, the ten samples were all tested for strength. The ratio of the strength of the five samples irradiated on both sides to the strength of the five samples irradiated on only one side was computed, and was found to be 0.99 with a standard deviation of 0.08.

Qualitative effects of irradiation

Before performing the quantitative strength tests of irradiated silk, it was subjected to high doses over an extended period of time, and imaged periodically to determine the impact on diameter (Fig. 5). The first visible damage to the silk occurs at around 1000 Mrad, which is far in excess of the anticipated 100 Mrad dose expected during the fill process. As the dose increased, the diameter of the silk decreased until the dose reached 4000 Mrad, after which there were no further visible effects on diameter. Although the diameter is slightly reduced by irradiation, this decrease is negligible for doses less than 500 Mrad. Therefore, properties that depend on the diameter (dose and stress) are computed using the unirradiated diameter of the silk.

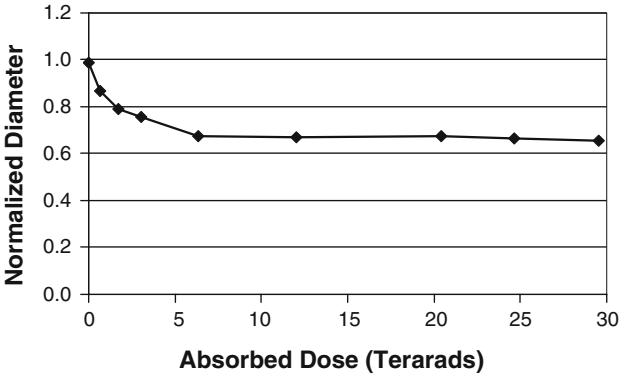

Fig. 5 Characterization of visible damage to silk samples as a result of high dose (as seen in SEM images). The diameter of the sample shrinks to about two-thirds of its initial diameter after exposure to a dose of about 6 Terarads, after which there is no further reduction in the diameter

Apparatus

The dragline sample (a segment of silk along with the two hollow, cylindrical handling tubes) is mounted vertically such that the lower end is held by a rigid steel pin, and the upper end is connected to a force transducer. The transducer moves upwards during a test, extending the sample. The unstressed length of the sample is typically between 25 and 26 mm.

Silk extension (and therefore strain) is controlled using a Zaber Technologies KT-HLA28 linear actuator, having an 0.8 μm step size, an adjustable rate, a maximum drive of 28 mm, and a maximum total error of ±4 μm over the full drive (including backlash). Since our experiments always proceed in the same direction, backlash is not an issue, and our uncertainty in position is less than a tenth of a micron. Our tests are conducted at a strain rate of 200 μm per second, and require less than a minute to complete. In a typical sample, the maximum strain ranges between 0.25 and 0.35.

The force in the silk is measured by a model 400A force transducer from Aurora Scientific. This device has a resolution of 5.4 μN, a maximum axial force of ±50 mN (and a

maximum side force of ±25 mN), and operates at 3300 Hz. In a typical strand of silk, the maximum force is 1.5 mN.

A typical run generates about 350 force-extension data pairs. Control and data acquisition are performed by a LabVIEW user interface, which monitors extension, force, and time for each measurement. The control system also records ambient air temperature, humidity, dose information, and the identity of the spider that generated the sample.

Since the silk remains attached to the handling tubes throughout a test, it is possible and even likely that the sample will be mounted so that the vertical strand is horizontally displaced from the centerline passing through the two mounting pins. Static friction from the mounting pins on the tubes usually prevents the resulting torque from rotating the mounting tubes, but sometimes the tubes slip and rotate. When this happens, there is an abrupt decrease in the force in the strand, which is apparent both onscreen to the system operator and in the resulting data set. In such cases, the test is aborted, and the data are not used.

Results

Factors affecting the strength of a sample include humidity, temperature, speed of harvest, and most importantly, spider size [4, 5]. Not only do bigger spiders generate larger silk, but heavier spiders generate proportionally stronger silk to support their increased weight. Also, individual segments of spider silk vary dramatically in strength, even silks from a single spider, and even segments that were originally adjacent on a single piece of dragline.

The four stress–strain plots shown in Fig. 6 are all generated from segments of a single piece of unirradiated dragline. The strength of samples from *different* spiders

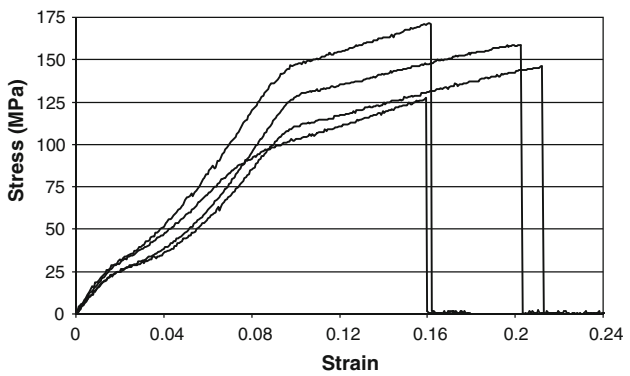

Fig. 6 Stress–strain relationship for four unirradiated silk samples from a single harvest. The strain is the independent variable. At failure (when the maximum stress is reached), several of the samples fall to 50% of the maximum stress, indicating that only one of the two strands has broken. The second strand breaks shortly afterwards, at a higher elongation

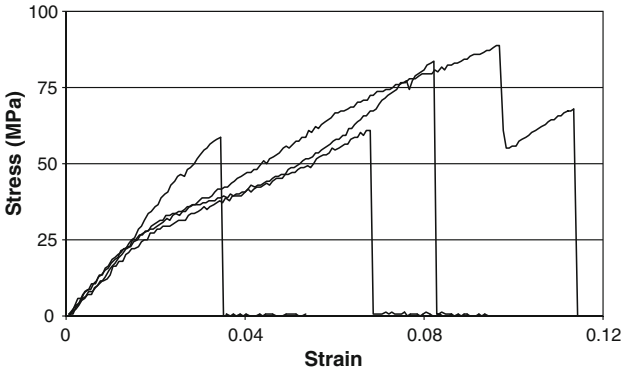

Fig. 7 Stress–strain behavior of four irradiated silk samples from the same harvest as Fig. 6. The exposure is 156 Mrad, and the average strength was reduced to 48% of the unirradiated strength. Note that the axes are scaled differently than in Fig. 6

varies from about 350 MPa, as shown here, to almost 2000 MPa. The plots shown here are typical, having two separate linear regions surrounding a curved region. The leftmost linear region is the "elastic" range, and indicates perfectly spring-like behavior. Both the stress and strain results for unirradiated silk compare favorably to that of Bonino [4], who used the same type of spider.

A set of typical stress–strain curves for both irradiated and unirradiated samples is shown in Fig. 7. One of these four samples shows clear evidence of the silk's double-stranded nature, where one of the two strands in the pair was noticeably tougher than the other. This behavior is noticeable about half of the time.

Tests with irradiated silk show a definite reduction in strength, toughness, and maximum extension before failure (Fig. 7). Unfortunately, since our samples are not irradiated over their full length, the strain results are a combination of the unirradiated and irradiated sections of the sample. As a result, the stain data cannot be used to compute secondary silk properties such as toughness, elasticity, or extension, since the strain of the irradiated portion of the sample is certainly less than the measured overall strain. However, the force is measured independently of the strain, and the maximum force (and stress) do not depend on the fraction of the silk that is irradiated.

As discussed earlier, ten samples are generated from each silk harvest. Five are tested without radiation, and the remaining five are irradiated and then tested. To determine the relative strength of the irradiated samples, the ratio of the average of the five irradiated samples to the average of the five unirradiated samples is computed. This ratio is plotted versus dose, which is composed of several hundred individual tests (Fig. 8). The uncertainty in the dose is estimated to be less than 10%, and is primarily a function of the uncertainty in the density of the silk (although fluctuations in the SEM current also contribute). The vertical uncertainties represent the standard deviation of each

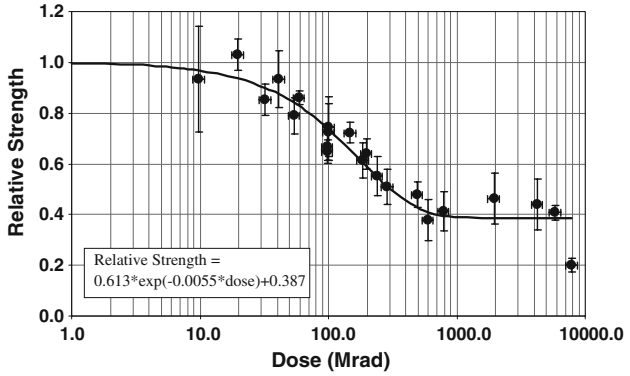

Fig. 8 Strength reduction as a function of dose. The impact of irradiation appears to be exponential. Relatively small doses (less than 10 Mrad) have minimal impact on strength. Doses higher than 8000 Mrad could not be strength tested because they became too brittle to mount onto the force transducer without breaking

computed result. At higher doses, the relative weakness of the irradiated silk resulted in many samples being accidentally destroyed during handling, so that the computed strength is the ratio of only one or two irradiated samples to five unirradiated samples.

As expected, the silk becomes weaker as dose increases. Using the method of least squares, the best fit exponential for this data results in:

$$\text{Relative strength} = [0.613 \pm 0.027] * \exp\left([-0.00554 \pm 0.00078] * \text{dose in Mrad}\right) + 0.387 \quad (2)$$

For the expected dose at LLE of 100 Mrad, this results in a relative strength of 74%. The dose necessary to reduce the strength to half of its initial value is around 300 Mrad. These results suggest that the use of silk as a means of securing the fusion targets remains a viable option for tritium targets that irradiate the silk.

Acknowledgements This work was funded in part by the US Department of Energy and the Laboratory for Laser Energetics. The authors would like to thank T. Craig Sangster and Mark Bonino of LLE for their assistance with issues related to ICF targets and spider silk handling. We would like to thank Dr. Anne Moore of the University of the Pacific for guidance in the measurement of force in spider silks. We would like to thank Clint Cross, Hui Jiang, and Bill Becker of SUNY Geneseo for assistance with equipment assembly, and testing. We would like to thank Dr. James McLean for assistance with calibration of the SEM.

References

1. Brinker BA et al (1983) J Vac Sci Technol A 1(2):941. doi: 10.1116/1.572158
2. Stephen Craxton R, McCroy RL, Soures JM (1986) Sci Am 255:68
3. Formation of deuterium ice layers in OMEGA targets (2004) LLE Review Quarterly Report, vol 99. LLE, University of Rochester, Rochester, pp 160–182
4. Bonino MJ (2003) Material properties of spider silk. Master's Thesis, Materials Science Program, The College School of Engineering and Applied Sciences, University of Rochester
5. Vollrath F, Kohler T (1996) Proc R Soc Lond B Biol Sci 263:387. doi:10.1098/rspb.1996.0059
6. Drouin D et al (2007) Scanning 29(3):92. doi:10.1002/sca.20000
7. Vollrath F (1999) Int J Biol Macromol 24(2–3):81. doi:10.1016/S0141-8130(98)00076-2
8. Ko FK et al (2002) Engineering properties of spider silk, Materials Research Society Symposium – Proceedings 702, pp 17–23
9. Saravanan D (2006) JTATM 5(1):1